Determination of Formation Constants and Specific Ion Interaction Coefficients for $Ca_nUO_2(CO_3)_3^{(4-2n)-}$ Complexes in NaCl Solution by Time-Resolved Laser-Induced Luminescence Spectroscopy.

Chengming Shang and Pascal E. Reiller

Den – Service d'Études Analytiques et de Réactivité des Surfaces (SEARS), CEA, Université Paris-Saclay, F-91191 Gif-sur-Yvette CEDEX, France.

Supporting Information

This supporting information contains 7 Figures and 4 Tables: the measured fluorescence emission spectra at atmospheric $CO_2(g)$, various Ca concentration and pH values, and 5 different ionic strength values; the predominance plots of the Ca-UO_2-CO_3 system under the experimental conditions; frequency distribution of the $\varepsilon(X^{2-}, Na^+)$ values from literature compared to the $\varepsilon(CaUO_2(CO_3)_3^{2-}, Na^+)$ determined in this work; and evolution of the saturation indices of calcite ($CaCO_3$), nesquehonite ($MgCO_3 : 3H_2O$), and dolomite ($CaMg(CO_3)_2$) from the theoretical speciation in Figure 9 of the main text; the stepwise formation constants values from Figure 5 of the main text; the $\varepsilon(X^{2-}, Na^+)$ values from literature.

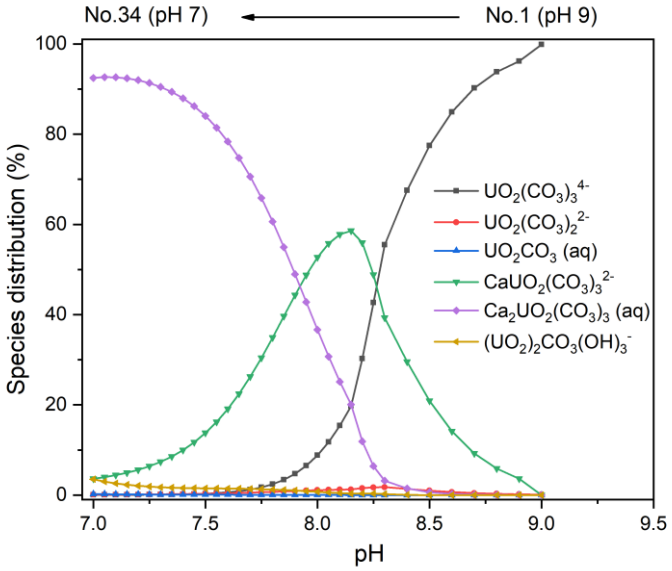

Figure S1. Species distribution at [U(VI)] = 50 μmol kg_w^{-1} in preliminary calculations with stability constants for $UO_2(CO_3)_3^{4-}$, $UO_2(CO_3)_2^{2-}$, $UO_2(CO_3)_3$(aq), and $(UO_2)_2CO_3(OH)_3^-$ listed in Table 1, and those for $Ca_nUO_2(CO_3)_3^{4-2n}$ taken from the work of Lee and Yun.[1] Other aqueous information is in Table S1.

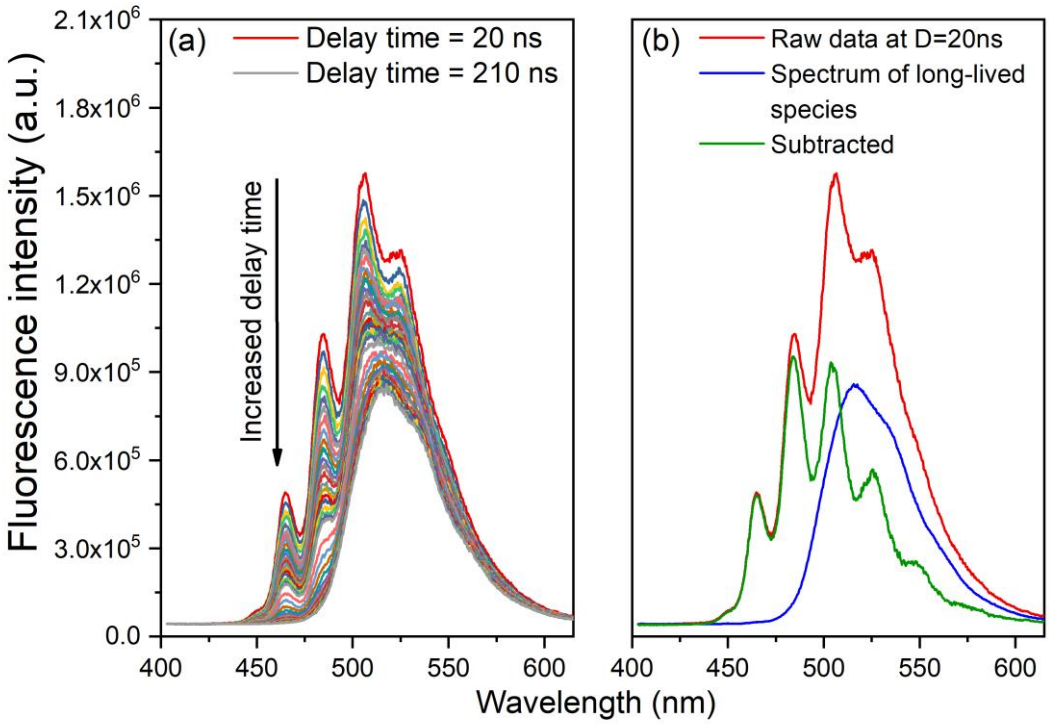

Figure S2. (a) Fluorescence decay spectra of the sample at [U(VI)] = 50 µmol kg_w^{-1}, pH = 7.6 equilibrated with atmospheric $CO_2(g)$, recorded with λ_{ex} = 450 nm from D = 20 ns to D = 210 ns. (b) Red line: spectrum recorded at D = 20 ns. Blue line: spectrum at D = 210 ns. Green line: subtraction of the blue line from the red one, also characteristic spectrum of UO_2-CO_3 species.

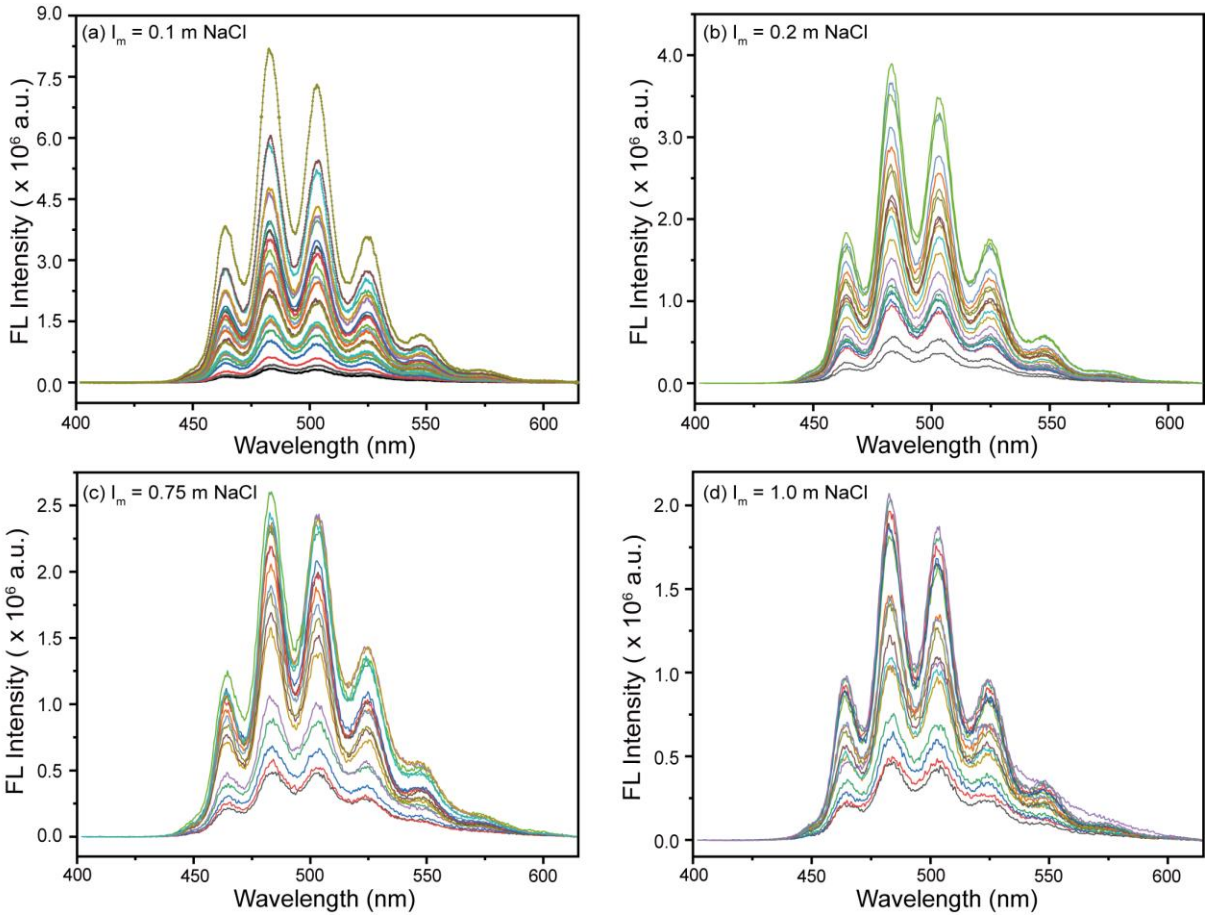

Figure S3. Measured fluorescence emission spectra of binary and ternary species at various calcium concentrations and pH values of (a) I_m = 0.1 mol kg_w^{-1}, (b) I_m = 0.2 mol kg_w^{-1}, (c) I_m = 0.75 mol kg_w^{-1}, and (d) I_m = 1.0 mol kg_w^{-1} NaCl series. Initial delay time D = 25 ns and gate width W = 1 μs, and 1000 accumulations fixed for all acquisitions.

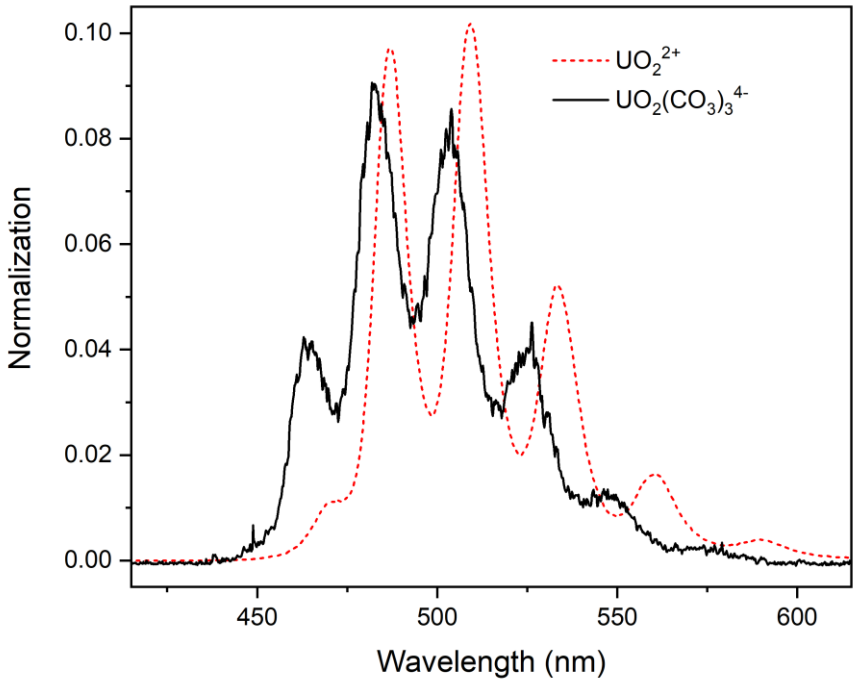

Figure S4. Hypsochromic-shifted fluorescence spectrum of $UO_2(CO_3)_3^{4-}$ ([U(VI)] = 50 μmol kg_w^{-1}, pH = 9, I_m = 0.1 mol kg_w^{-1} NaCl) compared with that of UO_2^{2+} ([U(VI)] = 0.1 mmol kg_w^{-1}, pH = 1) in $HClO_4$.

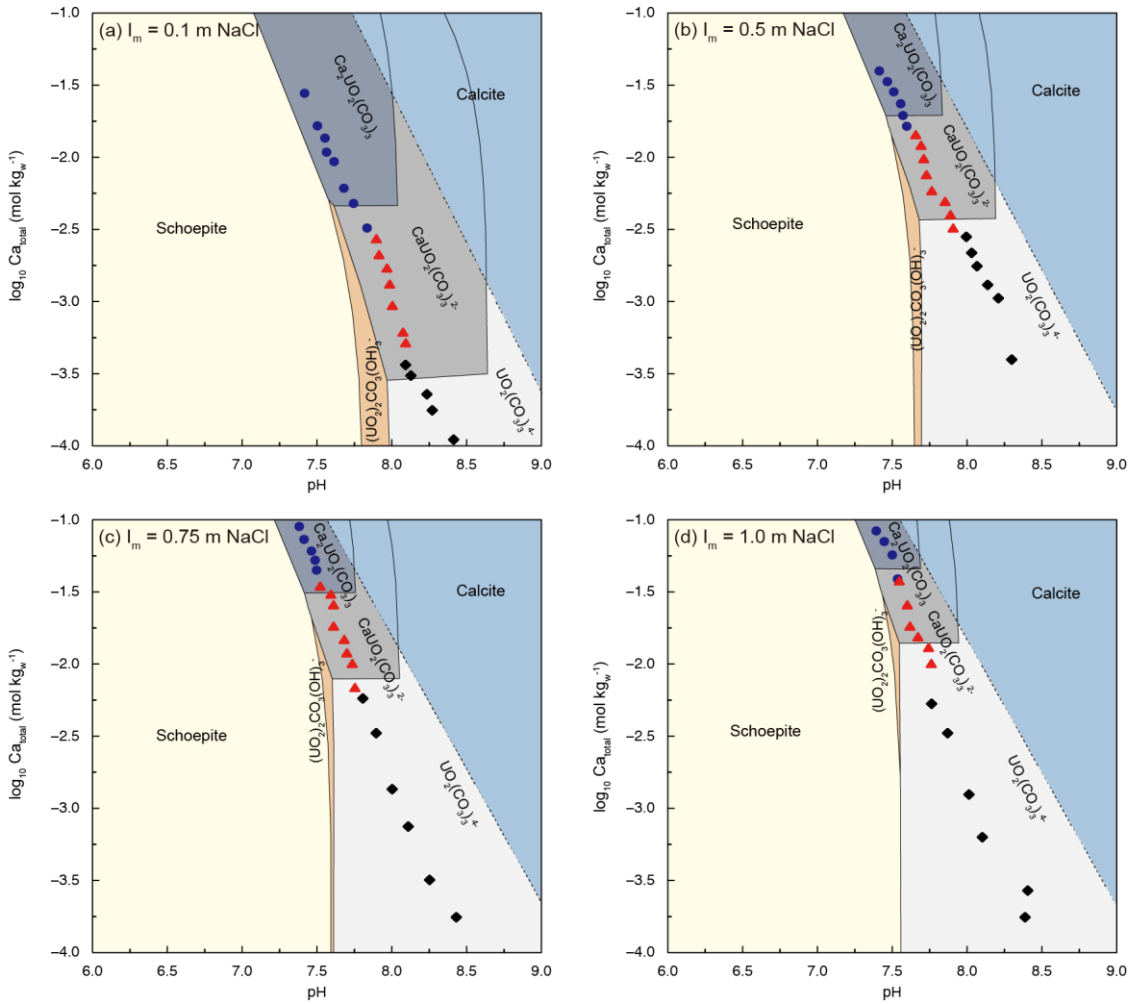

Figure S5. Predominance plots of Ca-UO_2-CO_3 system at [U(VI)] = 50 µmol kg_w^{-1}, $P(CO_2)$ = $10^{-3.5}$ atm and (a) I_m = 0.1 mol kg_w^{-1}, (b) I_m = 0.5 mol kg_w^{-1}, (c) I_m = 0.75 mol kg_w^{-1}, and (d) I_m = 1.0 mol kg_w^{-1} NaCl. Experimental points giving slopes of 1 and 2 are highlighted with red triangles and blue filled circles, respectively. The black diamond represents the beginning of titration where the binary complexes dominated.

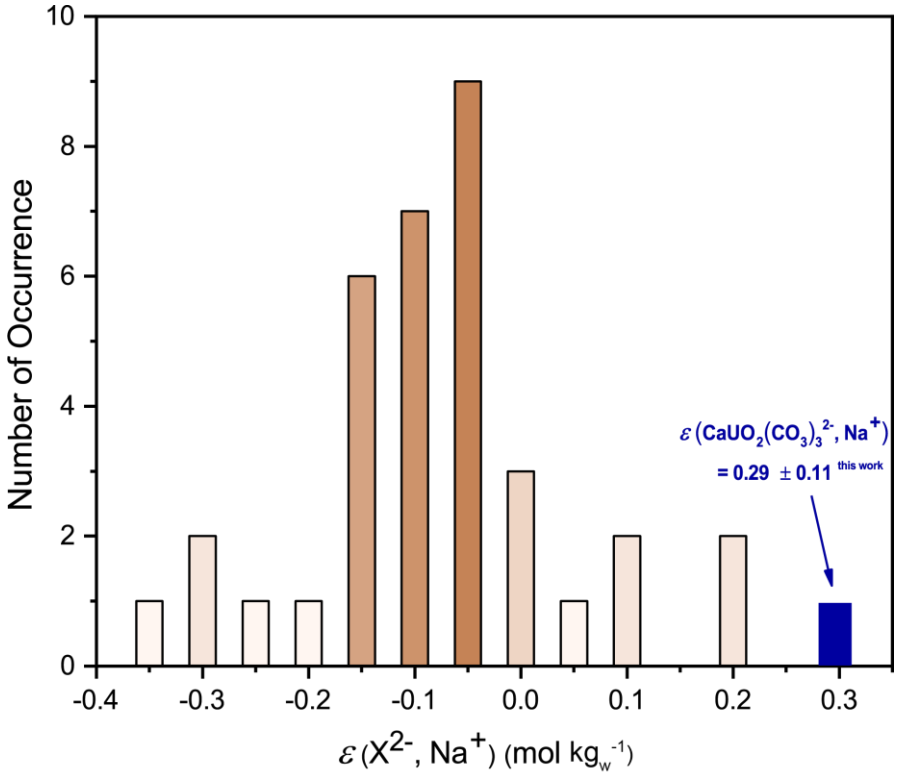

Figure S6. Frequency of the $\varepsilon(X^{2-}, Na^{+})$ from literature (**Erreur ! Source du renvoi introuvable.**); the values for $\varepsilon\left(Th(OH)_y(CO_3)_z^{4-y-2z}, Na^{+}\right)$ complexes[2] were not taken into account as they as they were proposed in analogy to like-charged complexes in [3] from data in NEA-OECD.[4-6]

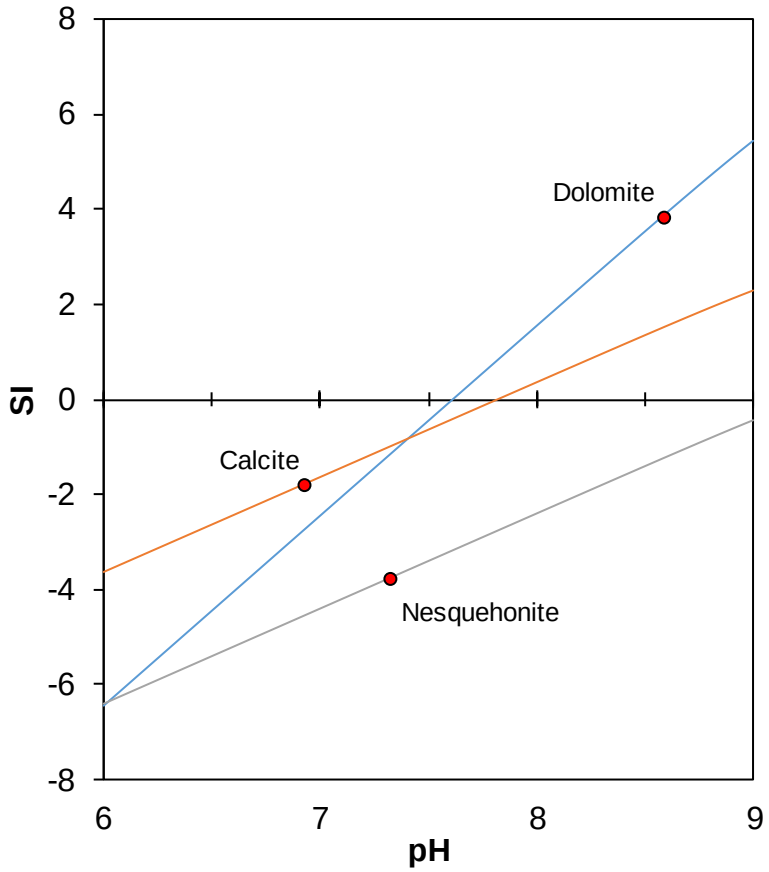

Figure S7. Evolution of the saturation indices of calcite ($CaCO_3$), nesquehonite ($MgCO_3 \cdot 3H_2O$), and dolomite ($CaMg(CO_3)_2$) from the theoretical speciation in Figure 9 of the main text.

Table S1. Aqueous conditions in preliminary calculations.

Sample No.	*pH*	*$log_{10}[Ca^{2+}]$ (mol kg_w^{-1})*	*$[Ca^{2+}]$ (mol kg_w^{-1})*
1	9.00	---	1.00×10^{-5}
2	8.90	-4.90	1.26×10^{-5}
3	8.80	-4.70	2.00×10^{-5}
4	8.70	-4.50	3.16×10^{-5}
5	8.60	-4.30	5.01×10^{-5}
6	8.50	-4.10	7.94×10^{-5}
7	8.40	-3.90	1.26×10^{-4}
8	8.30	-3.70	2.00×10^{-4}
9	8.25	-3.50	3.16×10^{-4}
10	8.20	-3.30	5.01×10^{-4}
11	8.15	-3.10	7.94×10^{-4}
12	8.10	-3.00	1.00×10^{-3}
13	8.05	-2.90	1.26×10^{-3}
14	8.00	-2.80	1.58×10^{-3}
15	7.95	-2.70	2.00×10^{-3}
16	7.90	-2.60	2.51×10^{-3}
17	7.85	-2.50	3.16×10^{-3}
18	7.80	-2.40	3.98×10^{-3}
19	7.75	-2.30	5.01×10^{-3}
20	7.70	-2.20	6.31×10^{-3}
21	7.65	-2.10	7.94×10^{-3}
22	7.60	-2.00	1.00×10^{-2}
23	7.55	-1.90	1.26×10^{-2}
24	7.50	-1.80	1.58×10^{-2}
25	7.45	-1.70	2.00×10^{-2}
26	7.40	-1.60	2.51×10^{-2}
27	7.35	-1.50	3.16×10^{-2}
28	7.30	-1.40	3.98×10^{-2}
29	7.25	-1.30	5.01×10^{-2}
30	7.20	-1.20	6.31×10^{-2}
31	7.15	-1.10	7.94×10^{-2}
32	7.10	-1.00	1.00×10^{-1}
33	7.05	-0.90	1.26×10^{-1}
34	7.00	-0.80	1.58×10^{-1}

Table S2. Calculated Ringböm coefficients α for experimental samples.

	I_m = 0.1 mol kg_w^{-1}		I_m = 0.2 mol kg_w^{-1}		I_m = 0.5 mol kg_w^{-1}		I_m = 0.75 mol kg_w^{-1}		I_m = 1 mol kg_w^{-1}	
Sample	pH value	α	pH value	α	pH value	α	pH value	α	pH value	α
1	9.00	1.00	8.98	1.00	9.00	1.00	9.05	1.00	8.94	1.00
2	8.66	1.06	8.45	1.00	8.42	1.01	8.45	1.00	8.40	1.01
3	8.42	1.04	8.28	1.02	8.32	1.03	8.24	1.01	8.44	1.04
4	8.26	1.10	8.21	1.04	8.17	1.04	8.10	1.01	8.12	1.03
5	8.23	1.12	8.18	1.04	8.12	1.02	8.02	1.02	8.04	1.03
6	8.15	1.24	8.16	1.06	8.10	1.03	7.90	1.06	7.85	1.04
7	8.11	1.37	8.14	1.06	8.07	1.05	7.83	1.12	7.77	1.13
8	8.10	1.34	8.13	1.07	8.02	1.05	7.79	1.19	7.83	1.06
9	8.08	1.51	8.05	1.10	7.91	1.11	7.75	1.29	7.73	1.20
10	8.00	2.06	7.93	1.59	7.89	1.15	7.70	1.53	7.66	1.46
11	7.97	2.52	7.90	1.88	7.83	1.27	7.62	2.28	7.60	1.85
12	7.92	3.30	7.85	2.42	7.76	1.63	7.57	2.94	7.55	2.38
13	7.87	4.79	7.82	2.90	7.72	1.97	7.53	3.94	7.52	3.04
14	7.85	5.51	7.77	4.05	7.69	2.31	7.50	4.85	7.48	3.86
15	7.81	7.07	7.75	4.73	7.67	2.57	7.45	6.95	7.36	9.08
16	7.75	11.55	7.73	5.42	7.66	2.73	7.40	10.15	7.32	12.31
17	7.63	28.25	7.64	10.60	7.65	2.91	7.35	14.87	7.28	16.98
18	7.60	37.08	7.57	18.27	7.60	4.01	7.31	20.34	--	--
19	7.55	53.34	7.54	23.09	7.54	6.16	7.28	25.78	--	--
20	7.52	70.02	7.44	50.93	7.49	8.89	7.24	35.42	--	--
21	7.50	79.91	7.36	98.01	7.41	16.67	--	--	--	--
22	7.48	96.30	--	--	7.38	21.02	--	--	--	--

Table S3. Stepwise formation constants derived from the rounded off slopes through the linear dependence of $\log_{10}R$ on $\log_{10}[Ca^{2+}]$ (mol·kg$_w^{-1}$).

I_m (mol·kg$_w^{-1}$)	$\log_{10}K_{113}$	$\log_{10}K_{213}$
0.10	3.58 ± 0.02	6.01 ± 0.03
0.20	3.17 ± 0.02	5.30 ± 0.03
0.50	2.50 ± 0.01	4.29 ± 0.02
0.75	2.16 ± 0.02	3.75 ± 0.01
1.00	1.95 ± 0.02	3.41 ± 0.03

Table S4. Values of the $\varepsilon(X^{2-}, Na^{+})$ from literature.

Species	$\varepsilon(X^{2-},Na^{+})$ $kg_w\ mol^{-1}$	References
$EdtaH_2^{2-}$	-0.37 ± 0.14	7
$UO_2F_4^{2-}$	-0.3 ± 0.06	4
ThF_6^{2-}	-0.3 ± 0.06	2
$Ni(Oxalate)_2^{2-}$	-0.26 ± 0.03	7
$UO_2(Edta)^{2-}$	-0.22 ± 0.18	7
$UO_2(Oxalate)_2^{2-}$	-0.18 ± 0.07	7
HPO_4^{2-}	-0.15 ± 0.06	4
ZrF_6^{2-}	-0.15 ± 0.06	8
$Mg(Oxalate)_2^{2-}$	-0.15 ± 0.03	7
$Si_2O_3(OH)_4^{2-}$	-0.15 ± 0.06	4
$Si_2O_3(OH)_4^{2-}$	-0.15 ± 0.06	4
$(UO_2)_2(OH)_2(SO_4)_2^{2-}$	-0.14 ± 0.22	4
$UO_2(SO_4)_2^{2-}$	-0.12 ± 0.06	4
SO_4^{2-}	-0.12 ± 0.06	4
$UO_2(N_3)_4^{2-}$	-0.1 ± 0.1	4
$Zr(OH)_6^{2-}$	-0.1 ± 0.1	8
$NpO_2(HPO4)_2^{2-}$	-0.1 ±	4
$SiO_2(OH)_2^{2-}$	-0.1 ± 0.07	4
$Th(SO4)_3^{2-}$	-0.091 ± 0.038	2
CO_3^{2-}	-0.08 ± 0.03	4
$Oxalate^{2-}$	-0.08 ± 0.01	7
SO_3^{2-}	-0.08 ± 0.05	4
$S_2O_3^{2-}$	-0.08 ± 0.05	4
CrO_4^{2-}	-0.06 ± 0.04	4
$Co(OH)_4^{2-}$	-0.06 ± 0.02	9
$NpO_2(Citrate)^{2-}$	-0.06 ± 0.03	7
$Fe(CO_3)_2^{2-}$	-0.05 ± 0.05	10
$CitrateH^{2-}$	-0.04 ± 0.02	7
$UO_2(CO_3)_2^{2-}$	-0.02 ± 0.09	4
$Mg(Edta)^{2-}$	-0.01 ± 0.15	7
$Zn(OH)_4^{2-}$	0.05 ± 0.04	11
$NpO_2(EdtaH)^{2-}$	0.07 ± 0.16	7
$Zn_2(OH)_6^{2-}$	0.1 ± 0.08	11
$Ni(CN)_4^{2-}$	0.185 ± 0.081	12
$Cu(OH)_4^{2-}$	0.19 ± 0.05	13

References

1. J. Y. Lee and J. I. Yun, *Dalton Trans.*, 2013, **42**, 9862-9869.

2. M. Rand, J. Fuger, I. Grenthe, V. Neck and D. Rai, *Chemical Thermodynamics 11. Chemical Thermodynamics of Thorium*, OECD Nuclear Energy Agency Data Bank, Eds., OECD Publications, Paris, France, 2009.

3. M. Altmaier, V. Neck, R. Muller and T. Fanghänel, *Radiochim. Acta*, 2005, **93**, 83-92.

4. R. Guillaumont, T. Fanghänel, V. Neck, J. Fuger, D. A. Palmer, I. Grenthe and M. H. Rand, *Update of the Chemical Thermodynamics of Uranium, Neptunium, Plutonium, Americium and Technetium*, OECD Nuclear Energy Agency, Data Bank, Issy-les-Moulineaux, France, 2003.

5. I. Grenthe, L. Fuger, R. G. M. Konings, R. J. Lemire, A. B. Muller, C. Nguyen-Trung and H. Wanner, *Chemical Thermodynamics 1. Chemical Thermodynamics of Uranium*, North Holland Elsevier Science Publishers B. V., Amsterdam, The Netherlands, 1992.

6. R. J. Lemire, J. Fuger, H. Nitsche, P. Potter, M. Rand, J. Rydberg, K. Spahiu, J. C. Sullivan, W. J. Ullman, P. Vitorge and H. Wanner, *Chemical Thermodynamics 4. Chemical Thermodynamics of Neptunium and Plutonium*, North Holland Elsevier Science Publishers B. V., Amsterdam, The Netherlands, 2001.

7. W. Hummel, G. Anderegg, L. F. Rao, I. Puigdomènech and O. Tochiyama, *Chemical Thermodynamics 9. Chemical Thermodynamics of Compounds and Complexes of U, Np, Pu, Am, Tc, Se, Ni and Zr with Selected Organic Ligands*, North Holland Elsevier Science Publishers B. V., Amsterdam, The Netherlands, 2005.

8. P. Brown, E. Curti, B. Grambow and C. Ekberg, *Chemical Thermodynamics 8. Chemical Thermodynamics of Zirconium*, North Holland Elsevier Science Publishers B. V., Amsterdam, The Netherlands, 2005.

9. N. V. Plyasunova, Y. Zhang and M. Muhammed, *Hydrometallurgy*, 1998, **48**, 153-169.

10. R. J. Lemire, U. Berner, C. Musikas, D. A. Palmer, P. Taylor and O. Tochiyama, *Chemical Thermodynamics 13a. Chemical Thermodynamics of Iron. Part 1*, OECD Nuclear Energy Agency Data Bank, Eds., OECD Publications, Paris, France, 2013.

11. Y. Zhang and M. Muhammed, *Hydrometallurgy*, 2001, **60**, 215-236.

12. H. Gamsjäger, J. Bugajski, T. Gajda, R. J. Lemire and W. Preis, *Chemical Thermodynamics 6. Chemical Thermodynamics of Nickel*, North Holland Elsevier Science Publishers B. V., Amsterdam, The Netherlands, 2005.

13. N. V. Plyasunova, M. S. Wang, Y. Zhang and M. Muhammed, *Hydrometallurgy*, 1997, **45**, 37-51.